JGR Biogeosciences

RESEARCH ARTICLE
10.1029/2025JG009630

Metagenomic Analysis of Thawing Permafrost Highlights Links Between Carbon and Nitrogen Cycling Processes in Abrupt Thaw Simulation

M. Laurent[1,2], M. R. Baysinger[1,2], A. Bartholomäus[3], T. Windirsch[1,4,5], J. Strauss[1], T. Sanders[6], S. Liebner[3,7], and C. Treat[1,8]

[1]Alfred Wegener Institute Helmholtz Centre for Polar and Marine Research, Permafrost Research Section, Potsdam, Germany, [2]University of Potsdam, Institute of Environmental Sciences and Geography, Potsdam, Germany, [3]GFZ Helmholtz Centre for Geosciences, Section Geomicrobiology, Potsdam, Germany, [4]University of Potsdam, Institute for Geosciences, Potsdam, Germany, [5]Research Institute for Sustainability Helmholtz Centre Potsdam, Potsdam, Germany, [6]Institut für Kohlenstoffkreisläufe Helmholtz-Zentrum Hereon, Geesthacht, Germany, [7]University of Potsdam, Institute for Biochemistry and Biology, Potsdam, Germany, [8]Center for Landscape Research in Sustainable Agricultural Futures, Aarhus University, Aarhus, Denmark

Abstract Abrupt permafrost thaw events are projected to contribute up to 40% of permafrost carbon (C) release to the atmosphere. They involve sudden hydrological shifts within the soil column; however, the exact microbial functional pathway shifts induced by these events remain cryptic. To investigate how C and nutrient cycling processes differ in thaw scenarios, we conducted metagenomic analyses in a pilot study on soil and water subsamples (two replicates per depth group, and treatment) after experimental thaw of intact soil columns (1 m tall mesocosms) and soil horizons in isolation (120 mL vial incubations). The microbial community structure response was masked by high depth dependency, with large shifts in functional pathways within the permafrost soil horizon under the "abrupt" treatment. Most pathways of C cycling remained similar under both "abrupt" and "gradual" thaw, while denitrification and sulfate functional pathways were stimulated within the "abrupt" treatment. This is likely caused by thaw water providing more energetically favorable terminal electron acceptors for metabolic pathways such as denitrification, thus inhibiting the terminal stages of C degradation that result in methane production. This is supported by the 90% decrease in CH_4 production under "abrupt" thaw simulation. This pilot study of "abrupt" and "gradual" thaw simulations highlights the potential for abrupt thaw to enhance carbon-nitrogen interactions by modifying redox conditions. Abrupt thaw events are expected to increase in warming permafrost regions, and results from our study offer a novel perspective on the close interactions that lowland permafrost soils have when cycling C and nutrients.

Plain Language Summary Palsas—a form of permafrost peatland that are small in size but rich in soil C—can either transition slowly into wetlands (gradual) or collapse (abrupt) in thermokarst ponds fast. The microbial response to the hydrological changes due to those two timelines is yet not fully understood. We simulated abrupt and gradual thaw scenarios in a laboratory incubation and took subsamples from the incubated soil (before and after the experiment). We found that the microbial community responded to thaw primarily in the permafrost soil horizon. From a previous experiment, we knew that carbon dioxide emission increased in abrupt thaw and that methane emission was negligible in "abrupt" in "gradual" thaw. By comparing the functional potential of the microbes, we were able to see "who" may be behind the previously observed carbon dioxide and methane patterns. These insights offer greater understanding, and promising future directions of inquiry into better predicting how permafrost will contribute to the greenhouse warming effect and global C cycle in our post-thaw future.

Key Points:

- Significant shifts in microbial community structure under abrupt thaw simulation in the Permafrost Layer only
- Functional pathways involved in C cycle were unchanged under "gradual" and "abrupt" thaw simulations, with the exception of methanogenesis
- Interactions with N cycle limited terminal steps of C cycle leading to methane production inhibition

Supporting Information:

Supporting Information may be found in the online version of this article.

Correspondence to:

M. Laurent,
melissa.laurent@awi.de

Citation:

Laurent, M., Baysinger, M. R., Bartholomäus, A., Windirsch, T., Strauss, J., Sanders, T., et al. (2026). Metagenomic analysis of thawing permafrost highlights links between carbon and nitrogen cycling processes in abrupt thaw simulation. *Journal of Geophysical Research: Biogeosciences*, *131*, e2025JG009630. https://doi.org/10.1029/2025JG009630

Received 11 DEC 2025
Accepted 13 FEB 2026

Author Contributions:

Conceptualization: M. Laurent, M. R. Baysinger, A. Bartholomäus, S. Liebner
Data curation: M. Laurent, M. R. Baysinger, A. Bartholomäus, T. Sanders
Formal analysis: A. Bartholomäus
Investigation: M. Laurent, M. R. Baysinger, S. Liebner
Methodology: M. Laurent, M. R. Baysinger, T. Windirsch, J. Strauss, T. Sanders, S. Liebner
Resources: S. Liebner

1. Introduction

Peatlands are major terrestrial carbon (C) sinks, primarily composed of partially decomposed organic matter (OM). Northern peatlands store approximately 415 ± 150 Pg of C, with 46% located in permafrost-affected regions, which are estimated to store 185 Pg C (Hugelius et al., 2020). Decomposition of C is limited due to frozen, and saturated soil conditions, allowing for large-scale C accumulation (Frolking & Roulet, 2007; Sannel & Kuhry, 2009; Turetsky et al., 2000). These C-rich permafrost peatland soils are of particular interest as the Arctic is warming three to four times faster than the global average, but the resilience of C to the conditions of a warming

Software: A. Bartholomäus
Supervision: J. Strauss, S. Liebner
Validation: A. Bartholomäus
Visualization: M. Laurent, M. R. Baysinger
Writing – original draft: M. Laurent, M. R. Baysinger
Writing – review & editing: M. Laurent, M. R. Baysinger, T. Windirsch, J. Strauss, S. Liebner

climate represents a large uncertainty in climate modeling efforts (Obu et al., 2019; Rantanen et al., 2022; Smith et al., 2022).

Palsas—peat mounds elevated by ice layers in the permafrost and surrounded by mire—are characteristic permafrost landforms of discontinuous permafrost zone lowlands (Seppälä, 1986). These permafrost formations hold cultural significance for local people, as well as varied ecosystem services, and particularly dynamic and C-rich soils (Markkula et al., 2019). However by the year 2080, its predicted that in a high-emission scenario, 98% of the current habitat that is suitable for palsa formation will no longer be able to maintain the environmental and climatic conditions that allow for palsas (Leppiniemi, 2025), with all other forms of permafrost across the discontinuous zone on a similar trajectory to extinction (Fewster et al., 2022; Leppiniemi, 2025).

Permafrost thaw sequences can be categorized as being "gradual" or "abrupt". Abrupt thaw is typically defined by its short timescale of thaw—days to years—compared to deepening of the active layer in gradual thaw, which occurs over years to decades (Turetsky et al., 2020). Although less frequent, abrupt thaw could contribute up to 40% of permafrost C emissions as climatic conditions shift (Turetsky et al., 2020). The greater C release expected during abrupt thaw could be partly explained by the high amount of organic C directly available to microbial decomposition (Serikova et al., 2018; Turetsky et al., 2020; Vonk et al., 2013). Recently, Webb et al. (2025) expanded the definition of abrupt thaw to include degradation within 30 years in ice-rich soils (>20%) and cases leading to permanent ecological change, emphasizing the role of environmental and hydrological disturbances. In palsas, the ice-rich soils and rapid degradation—leading to the formation of thermokarst ponds—monitored in Fennoscandia suggest that abrupt thaw is the dominant process (Borge et al., 2017; Leppiniemi, 2025; Verdonen et al., 2023). Hence, integrating hydrological processes into studies of abrupt thaw and C degradation is essential for understanding better permafrost C dynamics in palsas.

In palsa mires, abrupt thaw processes are observed in the collapse of ice-rich permafrost domes into the surrounding to thermokarst ponds, and post-thaw wetlands. These resulting post-thaw thermokarst ponds are known to be biochemically complex (In 'T Zandt et al., 2020; Leroy et al., 2025; Vonk et al., 2015) and potential "hotspots" of methane (CH_4) and carbon dioxide (CO_2) production, as found in recent flux measurement campaigns (Kuhn et al., 2018; Walter Anthony et al., 2016). Permafrost thaw also re-introduces nitrogen (N), sulfur (S), and iron (Fe). This represents a significant potential to stimulate microbial activity at all depths, particularly in nutrient-limited wetland soils (Patzner et al., 2020; Reddy & DeLaune, 2008). However, rapid environmental changes could also lead to a high stress for the microbial communities and therefore exterminate narrow guild communities such as methanogens (Ernakovich et al., 2022). Microbial analysis offers insight into the biology behind OM decomposition, and offers potential for mechanistic understanding to bridge this knowledge gap of global C estimate uncertainties.

Studies investigating soil-microbe interactions along natural thaw gradients—from intact palsas to fens—have measured shifts in methanogenic communities that drive increased CH_4 production and emissions in thawed environments (Freire-Zapata et al., 2024; Patzner et al., 2022; Woodcroft et al., 2018). Recently, they have also demonstrated a strong link between C release and parent vegetation (Baysinger et al., 2025). However, these findings primarily reflect biological processes occurring over several decades in relatively stable environments. In contrast, little is currently known about short-term microbial changes—both in community composition and functional pathways—under conditions of abrupt thaw, even though such thaw events in permafrost peatlands (as well as in other non-wetland permafrost regions like the ice-rich yedoma domain (Strauss et al., 2017; Strauss et al., 2022, 2024) are considered potential C "hotspots". These tiny organisms are adapted to the extreme conditions of life for these high-latitude soils, but the open question remains as to how these communities respond to the massive physiochemical shifts in their environment as frozen soil thaws abruptly to saturation (Mackelprang et al., 2016; Waldrop et al., 2025).

To compare C and nutrient cycling in gradual versus abrupt permafrost peatland thaw, we conducted two laboratory experiments where we thawed permafrost soils. We used whole-core mesocosms and vial incubations and simulated hydrological conditions of each thaw type. In line with Turetsky et al. (2020), "abrupt" thaw was defined as the sudden inundation of soil by water from thermokarst ponds forming around thawing palsas. In early work using vial incubations, removing vertical soil dynamics revealed a 90% reduction in CH_4 emissions from palsa permafrost soils under "abrupt" thaw, as compared to controls (Baysinger et al., 2025). In the companion papers to this study, researchers observed that "abrupt" thaw simulations resulted in an increase in net CO_2 emissions from palsa soils, but the dynamics driving this uptick in emissions was unclear (Laurent et al., 2025).

These findings suggest that there are likely unrecognized mechanistic processes within abrupt thaw sequences that differ from those associated with active layer thickening (gradual thaw). The formation of thermokarst ponds due to permafrost degradation establishes a hydrological, chemical, and (potential) microbiological continuum between intact permafrost soils and newly formed thermokarst ponds (Leroy et al., 2025; Peura et al., 2020). This continuum represents in significant stressors and opening of new environmental niches in microbial community structure (MCS). Recent studies have emphasized the critical role of this hydrological connection in mediating interactions between C and nutrient cycles, which, in turn, shape MCS and influence GHG emissions (Leroy et al., 2025; Patzner et al., 2020). However, to our knowledge, no research has yet investigated shifts in microbial functional pathways in the context of the net emission of greenhouse gasses resulting from abrupt thaw. Here, we use a metagenomic approach to sample all the microbial organisms within soil and water samples to understand the abundance of species, and the functional potential of these organisms. By combining these methods (laboratory incubations measuring GHGs, metagenomic analysis), we are able to test the hypothesis that the "abrupt" and "gradual" thaw scenarios utilize distinct functional pathways to decompose OM, which can be reflected in resulting GHG emissions. By exploring both thaw scenarios with metagenomic analysis from subsamples at each depth, we aim to connect how the enhanced CO_2 fluxes measured in the above-mentioned "abrupt" simulation may have been influenced by conditions that shifted in favor of alternative metabolic pathways.

2. Materials and Methods

2.1. Study Site

Samples were collected from a palsa-mire in a discontinuous permafrost area in Finnish Sápmi (Peera Palsa —68.8778°N, 21.0793°E). The landscape is glacially imprinted; the topography is characterized by low-lying orogenic zones, and depressions. The former are composed of moraines from the Pleistocene glaciations and bedrock ridges, while the latter are occupied by palsa-mires (Borge et al., 2017). The peatland inception began in 8,000–10,000 cal.yr BP (Ruppel et al., 2013) followed by permafrost aggradation in 3,400–1,800 cal yr. BP (P. O. Oksanen et al., 2003). The Peera palsa-mire-complex is composed of four palsas (Verdonen et al., 2023) surrounded by fens. The active layer is up to 60 cm thick and the peat layer reaches 1.7 m depth. In this study, we focused on the southernmost palsa plateau of this site (Figure 1). Aerial imagery was used to document the loss of 80% of Peera palsa's total area between 1960 and 2020 (Verdonen et al., 2023). The abrupt thaw sequence resulted in the formation of small ponds and thaw slump on the edges the palsa, bordering the surrounding mire (Figure S1 in Supporting Information S1). The vegetation on the palsa is characterized by *Betula nana subsp*, *Empetrum nigrum subsp* and *Vaccinium myrtillus*, and the surrounding mire is largely composed of floating mats of *Sphagnum* mosses, *Eriphorum angustifolium* and *Carex rostrata*. For more detail on vegetation, refer to Karlgård (2008); Malmer et al. (2005). The mean annual air temperature measured at the Kilpisjärvi station is −1.7°C and the average precipitation per year is 546 mm (1991–2020, FMI, 2024).

2.2. Soil Sampling

In this study, we used soil samples collected in the fall of 2022 and winter of 2023. We used the samples from the fall expedition to characterize the in situ MCS and functional pathways. The samples collected in winter were incubated and analyzed for geochemical parameters (see Section 2.4) post-incubation. During the fall expedition, soil cores were collected after the first frost of the year (mid-September 2022). Soil cores were brought to the surface and subdivided into three soil horizons: surface horizon (0–10 cm) - middle horizon (30–50)–permafrost (55–70). Henceforth, the depth groups referenced in this manuscript as defined as follows: the "Top" 10 cm from the surface, the Permafrost Table (PT) "PT" for organic soils in the middle of the soil column directly above the deepest soils—the PL "PL" with a max depth of 111 cm below surface (for more, see Table S2 in Supporting Information S1). Three replicate cores were collected to account for the spatial heterogeneity of the palsa site. The soils were largely organic histosols, with the top 20 cm composed of a Sphagnum-rich peat layer. For more detailed descriptions of each horizon, see (Baysinger et al., 2025). Active layer ("Top" and "middle" soil horizons) were carefully collected with a bread knife. The PL was sampled with a Snow, Ice, and Permafrost Research Establishment (SIPRE) auger (Jon's Machine Shop, Alaska, USA).

Soil cores for mesocosm incubations were collected in mid-winter (March 2023). The expedition was scheduled during winter to preserve in situ moisture conditions and prevent soil compaction by sampling when the ground was fully frozen, thereby minimizing disturbance to interactions between soil horizons. We collected 12 replicate

Figure 1. (a) Location of field site (Peera palsa—marked by large blue point) in relation to permafrost distribution across Fennoscandia and Russia (b) Aerial view of Peera palsa in 2021. The red line delimits the aerial extend of Peera palsa in 2021, the orange squares indicate the soil samples collected in autumn 2022 and the light blue circle the coring location of samples collected in winter 2023. (a) *Source*: GRID-Arendal; data from International Permafrost Association, 1998; (b) *Source*: University of Eastern Finland Geosciences Lab 2021 (Verdonen et al., 2023).

cores of one m from the palsa—six of which were used in this study for mesocosm experiments—and one additional long core extending to the mineral soil for sedimentary analysis. The cores were drilled using a SIPRE corer, wrapped in specialized foil, and stored frozen at −20°C.

Additionally, we collected 45 L of water from a thermokarst pond adjacent to the palsa. The ice cover was drilled using the SIPRE corer, and the water was stored in pre-cleaned 10-L canisters. Samples from both expeditions were stored at −20°C at the Kilpisjärvi Research Station during the expedition. They were later shipped frozen to AWI in Potsdam, Germany, in a refrigerated truck and stored at −20°C until the start of the experiment.

2.3. Incubation Setup

Soil cores in mesocosm columns were incubated under dark conditions at 10°C for 12 weeks in a custom-made incubator. The headspace of the mesocosm columns was flushed with ambient air. The mesocosms were sequentially thawed over the course of the incubation. To ensure fluxes between cores were comparable and not influenced by potential dying plants, we removed the surface vegetation. Therefore, we did not include the influence of plants in this setup, and used dark incubation to prevent eventual plant growth and photosynthesis.

To experimentally replicate permafrost thaw, the mesocosoms were first thawed to 60 cm below soil surface (active layer depth). The active layer (or thaw depth) was deepened every 4 weeks after by 20 cm at each step.

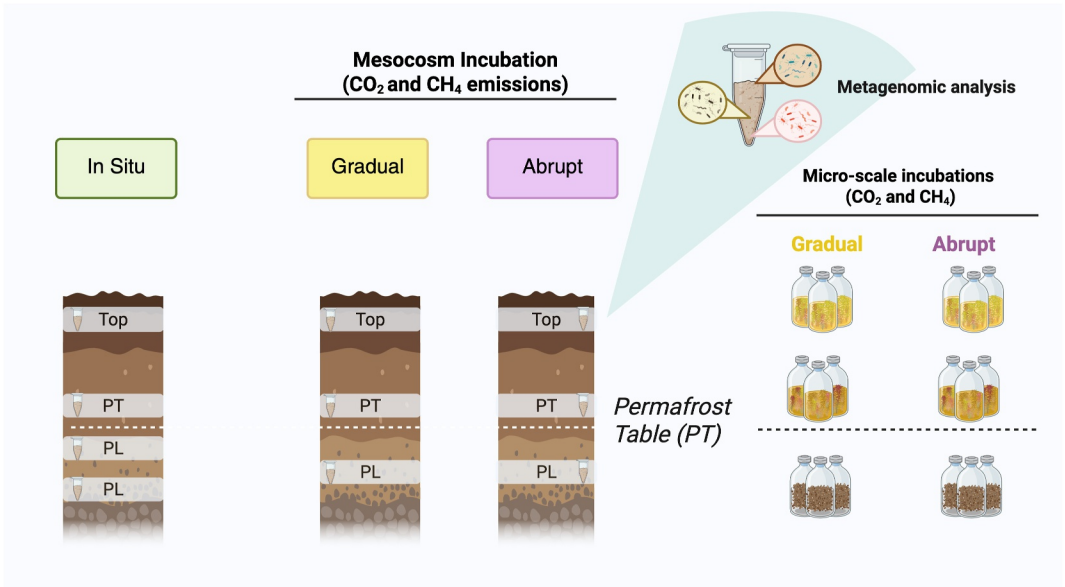

Figure 2. Schematic of the mesocosm setup used for incubation and the sampling depths (Top: 0–10 cm; Permafrost Table: 30–50 cm; Permafrost Layer: 60–90 cm) for metagenomic analysis. "Gradual" thaw refers to samples incubated under in situ soil moisture conditions, while "abrupt" thaw indicates samples that were flooded with thermokarst pond water. Microbial samples were sampled exclusively from the mesocosm incubations, while C release data from both incubation types were included in the discussion. For each microbial sampling layer (indicated in gray on the schematic), two biological soil replicates were sampled for metagenomic analysis, for a total of 20 soil samples. The last two biological replicates from the thermokarst lake are not shown here. Created with Biorender.

Temperature was monitored inside the incubator as well as along the soil profile. The temperature was recorded at five depths (0-20-40-60-80 cm) every half an hour by using HoBo sensors (Hobo U12-008 data logger, USA).

To assess the shifts in MCS and functional groups during abrupt and gradual thaw, we exposed the mesocosms to two treatments. We flooded a set of mesocosms to the surface with water from the thermokarst pond in order to simulate the collapse of the palsa into the pond (abrupt thaw). To simulate gradual thaw, we incubated the mesocosms at in situ soil moisture. For the "abrupt" treatment, the water was added from side at five depths (2–25–50–75 cm). Water was added bi-weekly and after each experimental thaw step and each water sampling (Laurent et al., 2025). Three replicate columns were used for each treatment, for a total of six mesocosms included in this study. Details regarding the mesocosm setup, the water preparation, water addition, as well as the incubation system are explained in Laurent et al. (2025). This work is linked to Baysinger et al. (2025). In Baysinger et al. (2025), three spatial replicate cores from four stages of permafrost thaw (delineated from vegetation, topography, and aerial imagery) were collected in the fall of 2023 from the same palsa sampled for this experiment–Peera palsa. The soil in Baysinger et al., was then incubated for a year in different headspace, temperature, and porewater treatments using 125 ml gas-tight vials of each soil horizon group (Figure 2). A summary of the GHG production findings from the "intact permafrost" thaw step (comparable to the permafrost collected for Laurent et al.'s mesocosms) can be found in Table 3.1.

2.4. Geochemistry Analysis

The sedimentary and geochemistry composition was analyzed (TOC, TN, electrical conductivity (EC), pH, water content) for the palsa site using a replicate core. Pore water for pH, EC and Dissolved Organic Carbon (DOC) was measured at every 10 cm. The pore water was extracted with a rhizon soil moisture sampler (Rhizon MOM 0.6 µm, Rhizosphere Research product–Meijboom and van Noordwijk, 1991). EC and pH measurements were conducted by a conductivity pocket meter with a reference temperature of 25°C (Cond 340i, WTW, Germany) and a potentiometer (Multilab 540, WTW, 125 Germany). The water for DOC was stored in 20 mL glass vials (WHEATON, Germany). To preserve the DOC, samples were acidified with 30% HCl (2 µL) and stored at 4°C prior analysis. The Total Organic Carbon (TOC), Total Carbon and Total Nitrogen (TN) were analyzed before and after incubation at five depths along the core (0–25–50–75–100 cm) with a Elementar soliTOC cube analyzer for

TOC and a rapidMAX N for TN (both from Elementar Analysen system, Germany). Each subsample was measured in duplicate, and standards and blanks were used to ensure reliable analytical measurements.

Pore water was collected at four depths (0–2 cm, 25 cm, 50 cm, and 75 cm) throughout the mesocosm incubation using rhizon moisture samplers prior to each thawing step (Laurent et al., 2026). Due to limited water availability, it was not always possible to collect sufficient volume for all chemical analyses (Table S5 in Supporting Information S1); as a result, complete data for N analysis are not available for all depths. Additionally, in the 'gradual' thaw treatment, where mesocosms were incubated under in situ soil moisture conditions, the upper 60 cm remained dry. Consequently, pore water was only collected from the PL at 75 cm depth in this treatment.

The pore water samples were stored frozen and were shipped to the Helmholtz-Zentrum Heron (Department Aquatic Nutrient Cycles, Geesthacht, Germany) for ammonium (NH_4^+), nitrate (NO_3^-) and nitrite (NO_2^-) concentration analysis. Nitrite and NO_3^- were determined by a HPLC method (Jasco) at 225 nm (Meincke et al., 1992). The detection limit was 0.5 µmol/L for NO_2^- and NO_3^-, respectively. Ammonium were determined by a photometric method and 609 nm (Hansen & Koroleff, 2007), the detection limit was because a necessary dilution 2 µmol/L.

2.5. Microbial Profile Analysis

Aliquots were taken for the metagenomic analysis both before (in situ) and after the mesocosm incubation. For each treatment (in situ, gradual and abrupt), we collected two samples (biological replicates) for microbial analysis in the top layer, at the PT and in the PL (Table S1 in Supporting Information S1). Our aim was to compare microbial community and functional changes during permafrost thaw. Because of the mesocosm setup, cores were collected in winter (see explanation above). As previous research shows strong microbial shifts between winter and summer (Deslippe et al., 2012; Poppeliers et al., 2022) and we did not want to capture microbial changes driven by seasonal thaw, we selected the cores collected in fall 2022 (when microbial communities had already transitioned to summer conditions but were still underlain by permafrost) to serve as the baseline. The other cores from winter 2023 were used for the permafrost thaw simulations.

Therefore for the "in situ" treatment, we analyzed samples from the homogenized soil horizons ($n = 3$ spatial replicate cores included in the homogenate) at four different depths (0–10 cm; 30–50 cm; 55–70 cm; 87–111 cm). Post-incubation samples were collected from the surface layer (0–2 cm), the transition layer between the active and the PL (50–55) and the PL (75–90).

The DNA extraction involved 0.5 g of soil following the PowerSoil DNA isolation kit protocol (Qiagen, Hilden, Germany). Before extraction, each biological replicate was homogenized individually to capture all variation from the replicates. For each biological replicate, we extracted DNA associated with the soil matrix in duplicate (DNA duplicates). DNA duplicates were mixed at the end of the extraction processes.

We generated 22 samples for DNA sequencing (Table S2 in Supporting Information S1). The quality and quantity of DNA were assessed fluorometrically using Genomic DNA ScreenTapes and High-sensitive RNA ScreenTapes on the Agilent 4150 TapeStation system (Agilent Technologies, USA) and Qubit 2.0 fluorometer (Thermo Fisher Scientific, United States). For metagenomic sequencing, Novogene GmbH (Planegg, Germany) conducted library preparation, and DNA sequencing on an Illumina NovaSeqX platform, targeting 50 million paired-end reads with a length of 150 nt.

2.6. Metagenome and Statistical Analyses

The metagenome data was processed using the ATLAS metagenome pipeline v2.12.0 (Kieser et al., 2020), which includes an extended workflow for quality control, contig assembly, gene prediction, functional annotation. Among the included tools are several standard tools, for example, metaSPAdes v3.15.3 for read assembly (Nurk et al., 2017), eggNOG mapper v2.1 and eggNOG database v5.0 for functional gene annotation (Cantalapiedra et al., 2021). Default parameters were used, except for RAM (up to 1.5 TB) and CPU/threads (up to 80 threads). We did not use MAG (metagenome assembled genomes) data created by ATLAS. Instead, we used a gene-centric approach and used all predicted and annotated genes for our analysis. The gene-centric approach usually gives a more complete picture, because a higher fraction of the total reads is represented by all genes compared to only the MAGs and its genes.

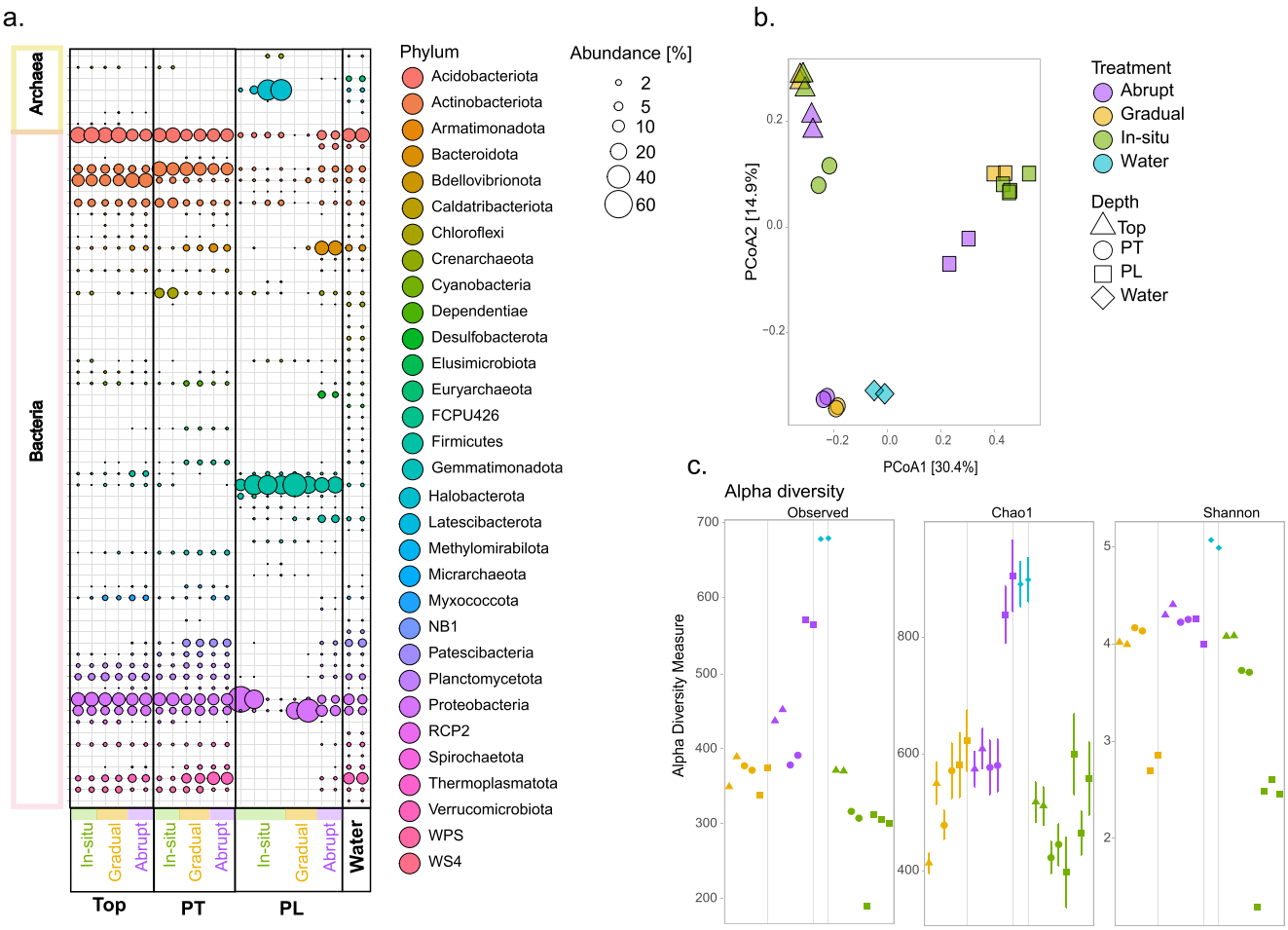

Figure 3. Microbial community structure across depths (Top: 0–10 cm; PT: 30–50 cm; PL: 60–90 cm) for samples collected before ("in situ": green), after incubation ("Gradual": yellow; "abrupt": purple) and for the thermokarst pond water (Water: blue). (a) Relative abundances of archaea and bacteria, with bubble size representing the relative abundance of each species and color indicating phylum identity. (b) Principal Coordinates Analysis based on relative species abundance. (c) Alpha diversity metrics, including Observed species, Chao1, and Shannon indices. In panels (b) and (c), point shapes represent different sampling depths.

The functional annotation with eggNOG also annotates KEGG orthology IDs (KOs). Table S8 in Supporting Information S1 includes all the corresponding genes and KO numbers that were part of the analysis corresponding to enzymes involved in C, N, iron and sulfur cycles chosen based on previous studies (Woodcroft et al., 2018). To create a general overview of the functional processes, we created a figure (4) similar to (Woodcroft et al., 2018). The detailed procedure is the following: (a) Gene counts for were normalized by calculating TPMs (reads per million mapped reads), where the total gene counts for each sample are the mapped reads. (b) TPMs for each pathway are summed for different KOs and KEGG pathways (for each sample separately). (c) Different pathways can have very different abundance, due to large range of genes involved and detected in each pathway. Thus, we scaled (i.e., divided) each pathways (i.e., each row in Figure 4) by the maximum value of this pathways. Thus, each row contains at least one value with 100% abundance. Please note, that we also considered using z-scale or mean scaling methods but without satisfactory results. This is likely caused by the different abundance pattern of different pathways (e.g., compare methanogenesis with only very few samples vs. glycolysis all samples showing gene abundance, Table S6, Table S9 in Supporting Information S1).

The differential gene abundance analysis was performed with the DESeq2 package (v1.34) (Love et al., 2014) to test whether gene counts differed significantly between sample groups. This analysis was done using the raw counts that were summed up by KEGG KOs/modules/pathways. DESeq2 fits a negative binomial model to the raw read count data, from which log2fold changes (treatment vs. control) were estimated. Significance was

determined using Wald tests with Benjamini-Hochberg correction, and features with an adjusted p-value <0.05 were considered differentially abundant.

Microbial community structure was characterized through taxonomic assignment for alpha- and beta-diversity analyses. The quality-controlled reads (from ATLAS, see above) were mapped to the SILVA rRNA database v138 (Quast et al., 2012) using Bowtie2 (Langmead & Salzberg, 2012) to quantify taxa in microbial communities (Figure S11 and Figure S12 in Supporting Information S1). Between 0.05% and 0.51% of the quality-controlled reads were successfully mapped to prokaryotic taxa in the SILVA database. To visualize beta-diversity, we conducted Principal Coordinates Analysis analyses, with inter-sample distances calculated using the Bray-Curtis dissimilarity metric from the vegan R package (J. Oksanen et al., 2020). We applied a PERMANOVA to test differences within depth, thaw treatment groups.

We performed data analysis and plot generation using R version 4.0.5 (R Core Team, 2021). Graphics were created using ggplot2 3.5 (Wickham et al., 2024).

3. Results

3.1. Greenhouse Gas Measurements From Multi-Scale Incubations

Over the incubation period (3 months), the mesocosms thawed under "abrupt" conditions emitted two-to three-fold more CO_2 than those under "gradual" conditions (Table 3.1). Under both thaw simulations, CH_4 uptake was observed, with no significant difference between treatments. N_2O emissions were similar during the initial thaw stages under both simulations (0.6 ± 1.19 and 1.82 ± 0.23 μg-N_2O m^{-2} h^{-1}). Although not statistically significant, N_2O emissions during the final thaw stage were higher under the "abrupt" thaw simulation.

The vial incubations exhibited a different pattern of GHG response, compared to the thaw simulations in the mesocosms. CO_2 production in the top of the active layer (0–15 cm) and middle active layer (15–32 cm) was similar under both thaw simulations. However, CO_2 production in the PL was reduced by 60% in the "abrupt" thaw simulation when compared to samples in the "gradual" thaw simulation (Table 3.1). Similarly, CH_4 production in the PL was reduced by a nearly 90% under the "abrupt" thaw simulation. In the 15–32 cm layer, the "abrupt" thaw simulation appeared to trigger CH_4 production, with a cumulative CH_4 production of 0.056 ± 0.1 mg-CH_4-C g^{-1} DW, compared to the absence of CH_4 under "gradual" thaw conditions (Table 3.1).

3.2. Microbial Community Structure

We generated 22 metagenomic libraries to characterize the MCS and the genetic functional potential. In total we obtained 2,528,005,914 raw reads that resulted in 1,351,484 assembled contigs (set of DNA segments that together represent the consensus pool of DNA) with 4,113,036,100 total bases (Table S7 in Supporting Information S1) and 2,276,819 predicted genes.

The depth at which the soil subsamples were collected was a major determinant of MCS. Significant differences were observed at both the phylum and family levels among the three depth groups ($P < 0.001$ for "Top" (0–10 cm) versus PL "PL" (60–90 cm), $P < 0.001$ for "Top" versus PT "PT" (30–50 cm), and $P < 0.001$ for "PL" versus "PT"; Figure 3b). The most prominent phyla within the soils of the active layer were Acidobacteriota, Actinobacteriota, Proteobacteria (20%–31%; Figure 3a, Table S3 in Supporting Information S1). In the lowest depth group (PL), the Firmicutes phylum was most dominant and represented 30% of the observed community (Figure 3a)

For both thaw simulations, the MCS from the 'PT' (30–50 cm depth) samples shifted toward the MCS of the thermokarst pond water. However, the experimental permafrost thaw simulations did not result in significant changes in the MCS between "gradual" and "abrupt" treatment groups (Figure 3b, Table S3 in Supporting Information S1). Within the lowest depth group (PL (55–90 cm depth)), only the MCS from samples exposed to the "abrupt" thaw simulation shifted toward the MCS of thermokarst pond water, while the MCS from samples incubated under "gradual" thaw remained similar to the "in situ" samples (Figure 3b). For example, we did not detect Bacteriodota in the permafrost layers prior to incubation, and Desulfobacterota were absent from all other soil samples. However, we detected both Bacteriodota and Desulfobacterota in the thermokarst pond water, where they accounted for 5% and 1.3% of the community, respectively. After the "abrupt" thaw simulation, we measured a relative abundance of 20% for Bacteriodota and 4% for Desulfobacterota in the permafrost layers, compared to

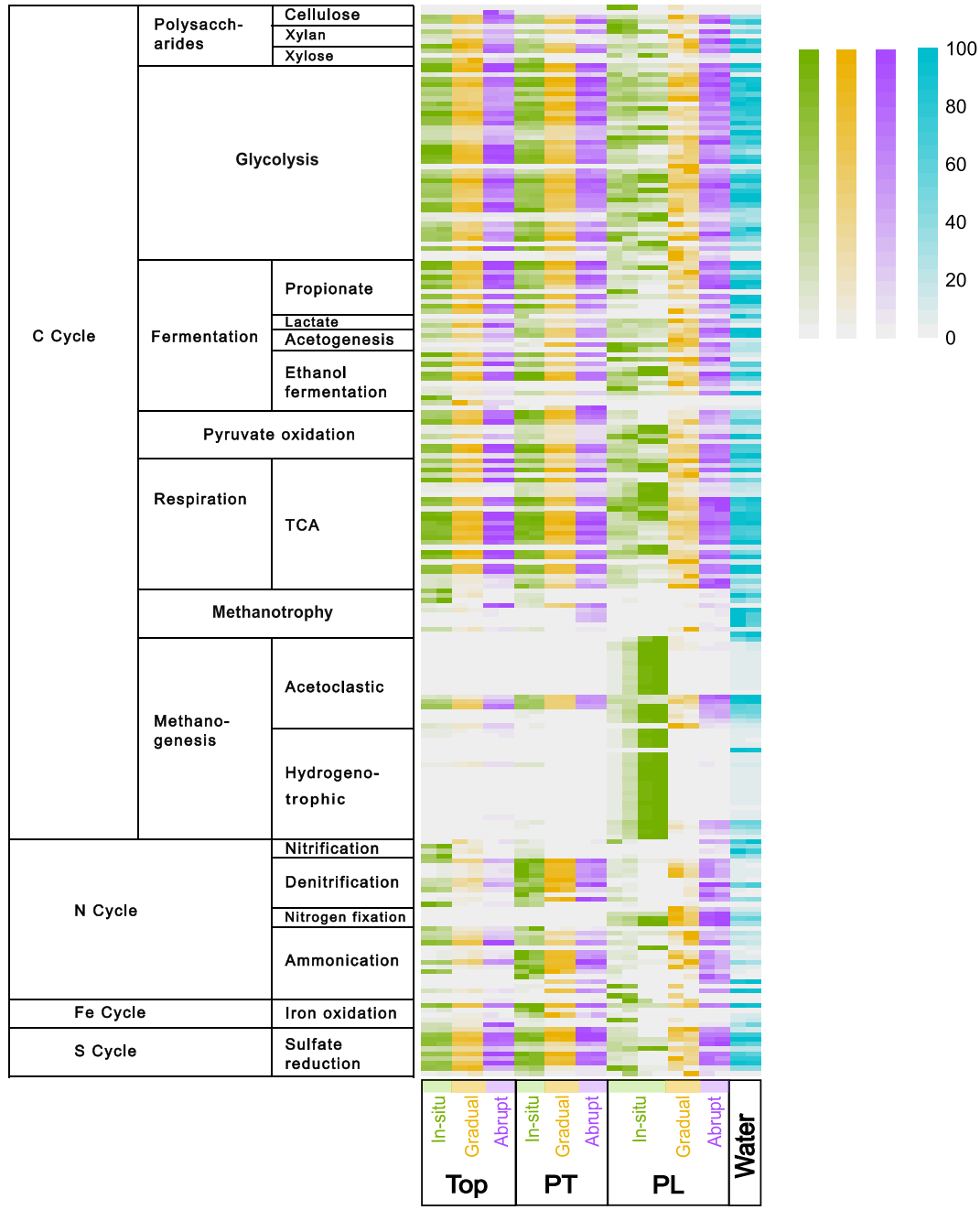

Figure 4. Heatmap showing the normalized abundance of KEGG Orthologs (KOs) associated with carbon (C), nitrogen (N), iron (Fe), and sulfur (S) cycling pathways across different depths (Top: 0–10 cm; PT: 30–50 cm; PL: 60–90 cm) for samples collected before ("in situ": green) and after incubation ("gradual": yellow; "abrupt": purple). The normalized abundances were obtained by calculated TPMs for each gene and sample followed by summing up by KOs and scaling each KO to the maximum of this KO (see methods for details).

just 1% and 0% under the "gradual" thaw simulation (Figure 3a, Table S3). Acidobacteriota was the most abundant phylum in the thermokarst pond water and was 100-fold higher in the "abrupt" than in the "gradual" thaw simulation (Figure 3a).

Phyla that had large shifts in abundance from "in situ" to the post-thaw simulation included the Bacteroida, Patescibacteria and Verrucomicrobiota phyla. These groups measured a sixfold increase after thaw, relative to the rest of the MCS (Figure 3a). Also notable was the Chloroflexi, which decreased by more than tenfold after both

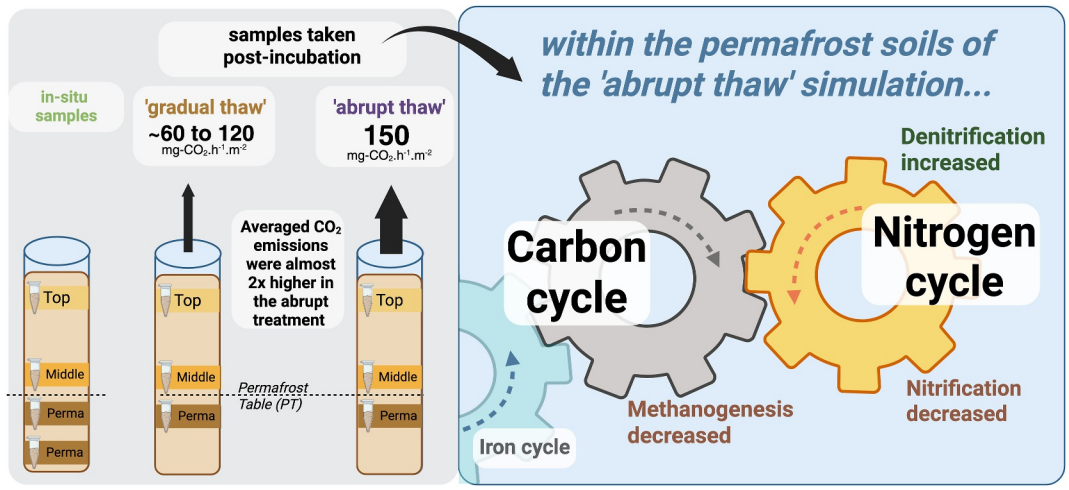

Figure 5. Displayed in the left panel is this study's experimental setup. Subsamples for metagenomic analysis are represented by the Eppendorf vials. Created with BioRender.

thaw treatments (Figure 3a, Table S3 in Supporting Information S1). No significant difference in MCS was observed within the "Top" depth group post-thaw (Figure 3b, Table S3 in Supporting Information S1). Finally, in the PL samples after the thaw simulations, Archaea were almost entirely absent (Figure 3a).

The thermokarst thaw water measured the highest biodiversity of any of the samples (see biodiversity indices Figure 3c). Within the water samples, no phyla had a relative abundance larger than 20% and most phyla represented in Figure 3a presented a relative abundance of 5% or less. Soil samples thawed under "abrupt" conditions had higher biodiversity indices independently of depths, with a stronger effect in the PL (Figure 3c). When the thermokarst water was introduced to soil in the "abrupt" thaw simulation, it was only in the PL depth group that the biodiversity indices increased (Figure 3c).

3.3. Functional Carbon Changes in the Permafrost Layer Following Thaw Simulations

Among the three layers analyzed for functional C cycle changes upon permafrost thaw, the "PL" layer was the only depth group with a shift in gene abundance between the "abrupt" and "gradual" thaw treatments (Figure 4). Methanogenesis genes using both the acetoclastic and hydrogenotrophic pathway were present in the "in situ" "PL" samples (Figure 4; Table 3.1) However, methanogenesis genes were not detected within all soil cores post-thaw treatment, but only within PL (Figure 4). The formation of acetate from pyruvate (acetogenesis) significantly decreased by a Log2FC of 1 and 0.6 for "gradual" and "abrupt" thaw respectively, but were still detected ($P < 0.001$, Table S4 in Supporting Information S1), while hydrogenotrophic pathway was not (Figure 4). Overall, acetoclastic pathway was detected in the post-thaw soil samples and thermokarst water. Both acetoclastic and hydrogenotrophic methanogenesis were only detected in the "in situ" PL samples (Figure 5).

The C cycle did not show a marked increase or decrease in response to "abrupt" thaw, though it was not entirely unaffected. From the metabolic functional data, we observed that a decrease in the genes associated with methanogenesis was the only overall response to thaw from the C cycle, despite the observed stimulation of GHG production (Table 3.1; $P > 2$ for all steps; Table S4 in Supporting Information S1). Glycolysis (pyruvate formation from glucose lysis) indicated some increase and decreases in individual steps of this metabolic pathway from the "abrupt" thaw simulation (Figure S9 in Supporting Information S1, $p = 0.017$) though the overall metabolic pathway was not significantly affected in "abrupt" or "gradual" thaw. Genes coding for polysaccharide degradation (degradation of polysaccharides such as cellulose or xylan to monosaccharides) were not affected by the type of thawing. In respiration and fermentation pathways there was no observed shift in gene abundances. Within the 'abrupt' thaw simulation, the gene abundances from the thermokarst water had a high correlation throughout the C cycle within the PL (Figures S2 and S3 in Supporting Information S1).

In the active layer ("Top" and "PT") soil depth groups, the metabolic pathways remained similar to those of the "in situ" group (Figure 4). Figure 4 displays shifts induced by thaw simulations solely for the methanotrophy, with

a overall increase in gene abundance under the "abrupt" thaw simulation. However, the TPM values (values normalized to gene length, and sequencing depth) for methanotrophy was low compared to the other pathways (median = 0.80, $Q1 = 0$, $Q3 = 10.70$, Table S6, Table S9 in Supporting Information S1), therefore the stronger abundance observed in Figure 4 is mainly attributed to the normalization used in the heatmap, rather than an absolute increase.

3.4. Varying Shifts in Nitrogen, Iron, and Sulfur Cycling Pathways in Response to Thaw Simulations

Based on the gene-centric analysis, we did not capture a clear functional response of the N pathways to the thaw treatments. Instead, each step in the N cycle did respond in some capacity to the treatments. These responses were depth-dependent, with the most significant differences originating from the "PL" depth group.

Although denitrification showed a stronger increase under "abrupt" thaw conditions (Log2FC = −1.6) than under "gradual" conditions (Log2FC = −1.05) in the "PL" depth group, this difference was not statistically significant (Table S4 in Supporting Information S1). Nitrification was completely inhibited in the "PL" after the "gradual" thaw simulation, as seen in Figure 4. Although we detected gene for this pathway under "abrupt" thaw, the TPM values were low. N fixation within the "PL" depth group was not significantly affected, and neither was ammonification. Although, thaw simulations significantly enhanced dissimilatory nitrate reduction, composed of denitrification and N fixation, by a Log2FC of −2.5 and −1.5 for "gradual" and "abrupt" thaw respectively ($P = 3.1E{-}6$ and 0.0019; Table S4 in Supporting Information S1). In the active layer ('Top'), the thaw simulations inhibited ammonification and nitrification, with a stronger inhibition for the 'abrupt' thaw simulation.

In contrast to the C cycling gene responses, the gene abundance of the "PL" under "abrupt" thaw was not correlated to that of the thermokarst pond water (Figure S7 in Supporting Information S1). The thermokarst pond water displayed the strongest gene abundance for the N fixation, ranging from 200 to 300 TPM. However, in comparison to the soil samples, the N cycle pathways in the thermokarst pond water have a lower gene abundance.

To gain another perspective of N cycling processes within the mesocosms, we extracted pore water samples at the end of the incubation and analyzed the different forms of N within the water. From these water samples, we found that both soil depth and thaw treatment influenced the N species concentration. Ammonium had the widest range in concentration (2141.7–3.6 μM; Table S5 in Supporting Information S1), with the highest levels found in deeper permafrost layers in the "abrupt" thaw simulation. Nitrate and NO_2^- generally were below the detection limit, with two exceptions from samples in the middle depths (both samples were around 5 μM; Table S5 in Supporting Information S1).

Gene abundances for the Fe and S cycles were also included in this analysis, but only one key pathway from each mineral/nutrient cycle is represented here: Fe II oxidation and sulfate reduction. While little to no change was observed for the iron oxidation, sulfate reduction increased (by a Log2FC of 1.4 for dissimilatory, and 0.84 for assimilatory; Table S4 in Supporting Information S1) under 'abrupt' thaw simulation. This increase in S reduction matches the gene abundance from the thermokarst pond water (Figure S8 in Supporting Information S1).

4. Discussion

4.1. Stability in Carbon Cycle Pathways Despite Microbial Structure Community Shifts

Functional pathways and MCS had little discernible changes within the active layer (Figures 3b and 4), likely as the high biodiversity of organisms within the soils, made for a population that could adapt to the changes thaw brought (Ernakovich et al., 2022). While the samples at the PT were undergoing the strongest MCS shifts for both simulations, no functional C shifts was measured (Figures 3b and 4). Similarly, the samples from the PL under "abrupt" thaw simulation showed a significant shift in MCS, but the functional C pathways were similar to "in situ" and "gradual" conditions (Figures 3b and 4, Yang et al. (2021)). This phenomena in the PL may possibly be explained by the ability of select groups of methanogens to maintain a relatively dormant—but still viable—life within the extreme cryogenic environment of the frozen soils (Mackelprang et al., 2017; Rivkina et al., 2007). Previous work at Stordalen Mire (using the top 50 cm of the active layer) found that fermentation processes shift mainly in the later stages of post-thaw wetland formation when the post-thaw wetland became an established fen, rather than during the entirety of the permafrost thaw sequence (Woodcroft et al., 2018).Whether soil is within the permafrost horizon, or in exchange with the atmosphere (active layer horizon) is one of the strongest drivers of MCS and functional potential (Waldrop et al., 2010). However, the absence of observed shifts in C cycling

Table 1
Summary Table of the Results From the Mesocosm and Vial Incubations for the "Gradual" and "Abrupt" Thaw Simulations

	Mesocosm incubation (3 months)				Vial incubation (1 year)		
	($mg\text{-}CO_2$ or $\mu g\text{-}CH_4$ m^{-2} h^{-1}, or $\mu g\text{-}N_2$ m^{-2} h^{-1})				($mg\ C\ g^{-1}$ DW)		
Thaw simulation	Thaw stage (cm)	Average CO_2 Emissions	Average CH_4 Emissions	Average N_2O Emissions	Incubation Depth (cm)	Average CO_2 Production	Average CH_4 Production
Gradual	0–60	56.6 ± 15.8	−10.8 ± 4.2	1.50 ± 0.367	0–15	2.73 ± 0.3	–
	0–80	32.8 ± 0.8	−3.2 ± 0.6	1.82 ± 0.23	15–31	2.08 ± 0.2	–
	0–100	98.3 ± 3.6	−15.5 ± 2.3	2.94 ± 0.96	54–61	1.12 ± 1.6	1.68 ± 1.1
Abrupt	0–60	178.8 ± 96.1	−18.1 ± 31.8	1.589 ± 1.39	0–15	2.58 ± 0.4	–
	0–80	96.1 ± 48.0	−27.9 ± 18.5	0.6 ± 1.19	15–31	2.66 ± 0.3	0.056 ± 0.1
	0–100	171.1 ± 90.4	−34.6 ± 15.4	35.7 ± 61.9	54–60	0.43 ± 0.01	0.192 ± 0.04

Note. Results from the mesocosm incubation indicate the average CO_2 and CH_4 emissions in $mg\text{-}CO_2$ or $\mu g\text{-}CH_4$ m^{-2} h^{-1} and N_2O emissions in $\mu g\text{-}N_2$ m^{-2} h^{-1} over individual thaw stage. Results from the vial incubation indicate the average potential cumulative production in $mg\text{-}CO_2$ or $mg\text{-}CH_4\text{-}C$ g^{-1} DW over a year of incubation. For both incubations, averages were calculated over three replicates.

functionalities (Figure 4) contrast with the increase in CO_2 emissions from palsa permafrost soils in the "abrupt" thaw simulation as compared to soils in a "gradual" simulation (Figure S10 in Supporting Information S1; Laurent et al. (2025)).

The MCS was mostly driven by the vertical soil distribution (Figure 3), consistent with previous knowledge. This result was expected, as the position of soil within or outside the permafrost horizon is well known to be a dominant control on microbial community composition and activity (Waldrop et al., 2010). Regarding changes due to thaw simulations, the functional pathways and MCS had little discernible changes within the active layer (Figures 3b and 4). This is likely due to the MSC already adapted to seasonal thaw. Additionally, this finding suggests C cycle functional pathways are broad enough to be carried by different MCS communities (Ernakovich et al., 2022). However, it could also indicate that MCS changes more rapidly than functional pathways.

The absence of observed shifts in functional genes (Figure 4) contrast with higher CO_2 emissions from the mesocosm under the "abrupt" thaw simulation (Table 1; Laurent et al. (2025)), as compared to soils in a "gradual" simulation. This indicates that other biochemical cycles could play a role in CO_2 release. As a next step, it could be valuable to use a transcriptomic approach in future work to quantify precisely which genes increased in response to 'abrupt' conditions, to explain our observed increase in CO_2.

Our 16S rRNA gene data supported a significant shift in MCS communities between the thaw simulations, with a shift toward the thermokarst pond water microbial community for the 'abrupt' thaw treatment in the PL (Figure 3b). This could indicate a potential colonization by microbial communities originating from the thermokarst water, as seen in the groupings (particularly of the abrupt "PL" samples) in (Figure 3b). There was an overall increased alpha-diversity in the samples under the "abrupt" thaw simulation (Figure 3c). In an incubation experiment testing the effects of higher microbial diversity on soil C respiration rates, Maron et al. (2018) measured a 1.5-fold increase in C decomposition with increased microbial diversity. When considering this in the context of our results, the relatively high microbial diversity in the thermokarst water carried over to the "abrupt" thaw simulation soils (see alpha diversity indices: Figure 3c), which could partly explain the two fold increase in CO_2 emissions measured in Laurent et al. (2025) (Maron et al., 2018). Furthermore, metagenomic analysis allows only for the identification of functional genes, but does not assess the activity of the microbial communities. Therefore, a potential higher activity due to a higher microbial diversity would not be captured here.

4.2. Potential Methane Inhibition Following Thaw

Functional gene abundance results combined with the CH_4 uptake from the mesocosm incubation suggest a potential inhibition of methanogenesis under 'gradual' and "abrupt" thaw conditions (Figure 4, Table 3.1). A decrease in gene abundance under "gradual" thaw is in line with previous studies, which reported reduced or no CH_4 production under drier conditions (Ernakovich et al., 2022; Knoblauch et al., 2018; Lee et al., 2012). As the

"gradual" thaw treatment was maintained at in situ moisture levels, it is likely that segments of the soil column experienced oxic conditions. However, despite water saturation, no CH_4 emission was measured and gene abundance corresponding to methanogenesis also decreased under the "abrupt" thaw treatment (Figure 4, Table 3.1, Table S4 in Supporting Information S1). In the companion paper Baysinger et al. (2025), both treatment groups were fully saturated though the "abrupt" group was incubated with thermokarst water from the site. In this yearlong incubation, the CH_4 production from permafrost soils were 90% lower than the soils that were incubated with the control treatment water (Table 3.1; Baysinger et al. (2025)).

Methanogens, characterized as a slow-growth ecological guild (Ernakovich et al., 2022), are known to respond stochastically (i.e., in random patterns) to environmental disturbances. Supporting this, Leroy et al. (2025) found that methanogens in emerging thermokarst lakes exhibited higher variability in behavior in a thawing palsa system in Canada. Our results support Leroy et al. (2025) that this observed pattern is likely due to the early developmental stage of these systems. Emerging thermokarst lakes may not yet provide the stable environmental conditions required for methanogen establishment. Their water chemistry, typically marked by low pH (Table S1 in Supporting Information S1; Leroy et al. (2025); Peura et al. (2020)), creates conditions that are unfavorable for the methanogenic organisms. This chemical bottleneck, despite otherwise likely favorable conditions (anoxic, warm), likely limits CH_4 production during early stages of abrupt permafrost thaw. The water samples from the thermokarst pond overall had a higher alpha diversity compared to the soil samples. However, from the water samples, methanogen abundance was below 2% and the gene encoding for methanogenesis were detected only for a few KOs compared to "in situ" conditions (Figures 3 and 4). This supports that water from young thermokarst ponds might be unfavorable to methanogenesis and aligns with the decrease in methanogenesis and gene abundance under abrupt simulation despite the flooded conditions. On the contrary, several studies have measured a high potential of CH_4 production from young thermokarst lake sediments (J. K. Heslop et al., 2019; J. Heslop et al., 2020). This highlights the complexity in thermokarst ponds and the different response to thaw between thermokarst pond sediments and thermokarst pond water. By flooding our palsa cores with thermokarst pond water, we only characterized the biochemistry effect from the thermokarst water, explaining why CH_4 release was contradicting other estimates from thermokarst lake sediments. It is also possible that the experimental setup may not have captured CH_4 created in the lower depths of the soil column, as it may have been oxidized in the surface soil layer, which is supported by the vial incubation data 3.1 but not corroborated with the microbial findings of this metagenomic analysis (Figure 3). When thinking about the discontinuous and sporadic permafrost systems, this finding supports that transitional stages in permafrost thaw are periods of dynamic system change, with aquatic (thermokarst pond) biogeochemistry having a widely underappreciated influence on GHG emissions from terrestrial soils.

While previous incubation studies have documented increased CH_4 production and methanogen abundance from post-thaw wetlands soils (Kirkwood et al., 2019; Mackelprang et al., 2011), they often relied on soil moisture as a proxy for anoxic conditions. However, Perryman et al. (2020) emphasized that redox potential is a more reliable predictor for some C processes in OM transformation during thaw transitions. The authors found that the redox conditions along the palsa thaw gradient of Stordalen mire was a more powerful predictor of CH_4 oxidation than the water table, as they measured anaerobic CH_4 inhibition under anoxic conditions—likely due to the utilization of other TEAs. Our gene centric-approach, combined with CH_4 production data from the vial incubations, is consistent with this perspective. In our 'abrupt' thaw simulations, we observed a modest increase in denitrification and significant increase in sulfate reduction-processes (Figure 4, Table S4 in Supporting Information S1) that could likely outcompete methanogenesis by using more energetically favorable TEAs (Reddy et al., 2022). The lower CH_4 production under 'abrupt' thaw compared to the 'gradual' thaw simulated in the vial incubation, further supports the preferential use of more energetically favorable TEAs. Finally, the absence of NO_3^- in pore water (Table S5 in Supporting Information S1) further supports our hypothesis that the intrusion of thermokarst pond water promotes denitrification as the primary energy-yielding pathway immediately following permafrost thaw. Methanogenesis is likely to become dominant later, once more favorable TEA pools have been depleted. This emphasizes the importance of incorporating local hydrological and geochemical conditions when assessing methanogenic dynamics. However, the limited sample size in our study constrains the broader applicability of these conclusions.

4.3. C-N Interactions Could Enhance Carbon Dioxide Production in the Abrupt Thaw Scenario

In the simulations of "abrupt" and "gradual" thaw presented here, there was no definite effect of the N cycle in response to different thaw simulations (Figure 4); rather, there were significant responses to thaw that were unique to each soil horizon and thaw stage. While this is a complex response, when considering each step in the N cycle individually some trends can start to be discerned from this pilot study of thaw processes. The environmental changes associated with permafrost thaw (increasing soil moisture, temperature) have been observed to enhance N cycling in high-latitude soils (Salmon et al., 2016). Recent work has linked this to diversification in N pathways used (Melillo et al., 2011; von Hippel et al., 2025).

Ammonification represents the transformation of organic N to more readily available forms of N - namely ammonia (NH_3) and ammonium (NH_4^+). In the water saturated conditions of the thawing permafrost cores in this study, genes indicating a functional potential for ammonification generally increased post-thaw simulation (Figure 4), though not to a statistically significant degree. However, a steady accumulation of ammonia was detected in the pore water of the mesocosm (Table S5 in Supporting Information S1); a telltale sign that the increase in genes indicating functional potential (Figure 4) was indicative of *actual* increase in activity of this step in the N cycle.

Genes indicating potential for nitrification were less present in the PL in both the "gradual" and "abrupt" thaw simulations (Figure 4). This aerobic process transforms NH_3 to NO_2^- and then to NO_3^-. Previous studies have found increases in nitrification following experimental thaw (Mackelprang et al., 2011), which is logical as it is largely a process that happens in the active layer of soils, constrained by the permafrost soil horizon (Wild et al., 2015). It was therefore interesting to note the reduced detection of nitrification and low NO_3^- and NO_2^- in the post-incubation pore water (Table S5 in Supporting Information S1). Soil pore water at all depths had NO_2^- below instrument detection limits for all depths. Nitrate concentrations were also below detection limit, except for some samples in the middle depths, with concentrations slightly higher detection minimum (Table S5 in Supporting Information S1). While terrestrial nitrification has been studied in a wide variety of soils (Booth et al., 2005), exploring how rates of nitrification change with thaw (and especially "abrupt" thaw) remain an open question with its significance highlighted in this study. Nitrogen fixation did not differ at any depth of the mesocosm cores between thaw simulation. For more on this terminal steps of the N cycle see Text 1 in Supporting Information S1.

We measured an overall increase in denitrification functional genes in all layers in the "abrupt" thaw sequence (Figure 4, Figure S9, Table S4 in Supporting Information S1). This process is promoted in anaerobic conditions, and spurs NO_3^- consumption within the soil matrix. Plants uptake two main N forms: NH_4^+ and NO_3^-—though the often N-limited boreal and arctic plants have been known to also uptake organic forms of N (Atkin, 1996). Therefore, a spurring of denitrification—as indicated in the 'abrupt' thaw scenario—may result in relatively less (bioavailable) NO_3^- within the soil column that plants and bacteria can most easily "consume". N_2O is produced at this step, anaerobically using NO_3^- as a TEA; notably, under complete anaerobic conditions, the N_2O is largely further reduced to N_2. Using soils from Peera palsa, Voigt et al. (2017) used a mesocosm setup to experimentally thaw the permafrost soil in 16-week thaw pulses. The authors found that total inundation (comparable to "palsa collapse" or "abrupt" thaw processes simulated in this manuscript) allowed for complete denitrification (reducing the produced N_2O to N_2 within the soil column) and thus tampering the GHG effect. The weak correlation in N pathway gene abundance between thermokarst pond samples and the "abrupt" "PL" treatment suggests that denitrification was not primarily driven by pond-derived denitrifiers (Figure S7 in Supporting Information S1). Instead, it was likely enhanced by increased soil moisture due to water addition and thaw of ice-rich permafrost. Previous studies have also found increases in denitrification following experimental thaw (Mackelprang et al., 2011). In our study, glycolysis was the only C metabolism pathway that had an enhanced overall detection in the early steps of the "abrupt" thaw scenario (Figure 4, Table S4 in Supporting Information S1). This is notable, as glycolysis produces NADH, a key electron donor for NO_3^- and NO_2^- reduction (Su et al., 2015), and may have triggered the observed denitrification response. However, NO_3^- and NO_2^- were nearly undetectable in pore water (Table S4 in Supporting Information S1), suggesting that limited horizontal transport of available N restricted broader C-N cycle coupling. It's also worth noting that while most of the pathways associated with glycolysis were overall enhanced, the one exception was the Entner-Doudoroff pathway (M00008 in Figure S9 in Supporting Information S1) which was not detected as having an enhanced detection.

While nothing indicates a metabolic shifts in the C cycle to explain the observed two-fold increase in CO_2 emissions during the "abrupt" simulation in the mesocosm incubation (Table 3.1); shifts in N cycles could indirectly influence CO_2 release (Monteux et al., 2020). Under anaerobic conditions, OM degradation can be coupled to alternative processes such as denitrification. This results in increasing anaerobic respiration and produces CO_2 as a byproduct (Reddy & DeLaune, 2008), which could also explained the observed increase in CO_2 emissions under the "abrupt" thaw simulation (Table 3.1). Sulfate was also observed as an alternative electron acceptor in sulfate reduction when soil moisture increases (Pester, 2012). In our pilot study, although gene abundance for sulfate reduction pathways did not change significantly following thaw, we measured an increase under the "abrupt" thaw treatment ($\log2FC = -1.4$; Figure 4) which may also contribute to higher CO_2 emissions (Table 3.1). Other studies associated enhanced CO_2 emissions to Fe reduction (Patzner et al., 2020, 2022). However, we did not see an enhancement of the gene abundance in the Fe cycle under the "abrupt" thaw simulation (Figure 4). A possible explanation could be the thick organic layer (2.10 m) at Peera palsa, compared to Stordalen (0.6 m), where this reaction was measured. The deeper mineral layer in Peera palsa likely prevents the Fe-OM interactions observed in Patzner et al. (2020) observations from Stordalen Mire.

4.4. Recommended Directions of Study, Toward Better Understanding C-N Interactions in Permafrost Thaw Sequences

This pilot study of thaw timeline on microbial metabolic processes emphasizes that the N dynamics of Peera palsa played a role in the resulting GHG emissions from simulated thaw sequences. Peera palsa is unique in its relatively thick peat layer. The results herein show that the functional pathways and MCS had little discernible changes within the active layer, likely as the high biodiversity of organisms within the soils allowed for a highly adaptable population (Ernakovich et al., 2022), while the permafrost soils were driven by factors entirely separate than that of the active layer. In using soils from one palsa, we are limited in the ability to extrapolate these results but rather provide novel suggestions and insights into the microbial workings of these soils. Though the microbial population and functional data interpretations and applications are in the early stages of this expanding field, it may soon be able to link MCS's directly to GHG production patterns (Li et al., 2025) and other relevant upscaling efforts. Further sampling campaigns using similar methods for field sites encompassing more of the discontinuous permafrost region—especially those influenced by abrupt thaw processes—would provide insight into abrupt thaw C dynamics and therefore reduce uncertainties in the contribution of permafrost C to the atmospheric C pool.

5. Conclusion

This study represents a first metagenomic analysis of functional group shifts linked to CO_2 and CH_4 releases as a result of abrupt thaw processes. By using mesocosm incubations, we preserved the in situ soil structure—an essential factor for the study of vertical soil dynamics. Our findings suggest that while C cycling functional pathways remained largely stable, shifts in N cycling, driven by the intrusion of thermokarst pond water, likely play a key role in regulating C release by altering terminal electron acceptor availability in the early stages of abrupt permafrost thaw.

Additionally, the higher microbial diversity observed in thermokarst pond water is likely to stimulate biogeochemical cycling. Our results highlight the importance of accounting for hydrological changes and soil-microbe interactions during abrupt thaw timelines. We call for increased attention on C-N interactions in permafrost peatlands. Especially for further investigations using thermokarst pond water, as the interaction between permafrost soils and these increasingly saturated habitats are critical in improving our understanding of short-term C release dynamics under abrupt thaw conditions.

Conflict of Interest

The authors declare no conflicts of interest relevant to this study.

Data Availability Statement

The metagenomics raw data has been deposited at the European Nucleotide Archive (ENA) under the project accession number PRJEB85523. Associated data generated within this project are archived in PANGAEA. Soil

data are available under: Laurent et al. (2023a) and Baysinger et al. (2023a) and Laurent et al. (2026). Incubation data are available under: Laurent et al. (2023b) and Baysinger et al. (2023b).

Acknowledgments
This study was funded by the Alfred Wegener Institute Helmholtz Center for Polar and Marine Research (AWI, grant details: INSPIRES PhD Fellowship to M.L.) and the European Research Council (ERC grant to C.T: FluxWIN Project 851181). We are grateful to the Research Station of Kilpisjärvi (University of Helsinki) for their assistance and support during fieldwork as well as the Sámi community for granting us permission to collect samples in culturally significant areas. We would like to acknowledge J. Vollmer, M. Dolle and S. Wocheslander, as well as the AWI and GFZ lab technicians, for their support with laboratory work. We also thank our colleagues for their valuable discussions and feedback. Open Access funding enabled and organized by Projekt DEAL.

References

Atkin, O. (1996). Reassessing the nitrogen relations of arctic plants: A mini-review. *Plant, Cell and Environment*, *19*(6), 695–704. https://doi.org/10.1111/j.1365-3040.1996.tb00404.x

Baysinger, M., Laurent, M., Verdonen, M., Reif, J., Kumpula, T., Liebner, S., & Treat, C. (2025). Abrupt thaw in a Finnish palsa: Potential ch4 production driven by vegetation adaptation in the transition from permafrost to post-thaw soils. *Journal of Geophysical Research: Biogeosciences*, *130*(9), e2025JG008847. https://doi.org/10.1029/2025jg008847

Baysinger, M., Verdonen, M., Kumpula, T., Reif, J., Laurent, M., Liebner, S., & Treat, C. C. (2023a). Geochemical measurements from permafrost soils across thaw stages in peera Palsa (finland) [dataset]. *PANGAEA*. https://doi.org/10.1594/PANGAEA.972636

Baysinger, M., Verdonen, M., Kumpula, T., Reif, J., Laurent, M., Liebner, S., & Treat, C. C. (2023b). Incubation of soils from across a permafrost thaw gradient [dataset]. In *Peera palsa (finland)*. https://doi.org/10.1594/PANGAEA.972634

Booth, M. S., Stark, J. M., & Rastetter, E. (2005). Controls on nitrogen cycling in terrestrial ecosystems: A synthetic analysis of literature data. *Ecological Monographs*, *75*(2), 139–157. https://doi.org/10.1890/04-0988

Borge, A. F., Westermann, S., Solheim, I., & Etzelmüller, B. (2017). Strong degradation of palsas and peat plateaus in northern Norway during the last 60 years. *The Cryosphere*, *11*(1), 1–16. https://doi.org/10.5194/tc-11-1-2017

Cantalapiedra, C. P., Hernández-Plaza, A., Letunic, I., Bork, P., & Huerta-Cepas, J. (2021). eggnog-mapper v2: Functional annotation, orthology assignments, and domain prediction at the metagenomic scale. *Molecular Biology and Evolution*, *38*(12), 5825–5829. https://doi.org/10.1093/molbev/msab293

Deslippe, J. R., Hartmann, M., Simard, S. W., & Mohn, W. W. (2012). Long-term warming alters the composition of arctic soil microbial communities. *FEMS Microbiology Ecology*, *82*(2), 303–315. https://doi.org/10.1111/j.1574-6941.2012.01350.x

Ernakovich, J. G., Barbato, R. A., Rich, V. I., Schädel, C., Hewitt, R. E., Doherty, S. J., et al. (2022). Microbiome assembly in thawing permafrost and its feedbacks to climate. *Global Change Biology*, *28*(17), 5007–5026. https://doi.org/10.1111/gcb.16231

Fewster, R. E., Morris, P. J., Ivanovic, R. F., Swindles, G. T., Peregon, A. M., & Smith, C. J. (2022). Imminent loss of climate space for permafrost peatlands in Europe and Western siberia. *Nature Climate Change*, *12*(4), 373–379. https://doi.org/10.1038/s41558-022-01296-7

Freire-Zapata, V., Holland-Moritz, H., Cronin, D. R., Aroney, S., Smith, D. A., Wilson, R. M., et al. (2024). Microbiome–metabolite linkages drive greenhouse gas dynamics over a permafrost thaw gradient. *Nature Microbiology*, *9*(11), 2892–2908. https://doi.org/10.1038/s41564-024-01800-z

Frolking, S., & Roulet, N. T. (2007). Holocene radiative forcing impact of northern peatland carbon accumulation and methane emissions. *Global Change Biology*, *13*(5), 1079–1088. https://doi.org/10.1111/j.1365-2486.2007.01339.x

Hansen, H. P., & Koroleff, F. (2007). Determination of nutrients. In *Methods of seawater analysis* (3rd ed., pp. 159–228). Wiley VCH.

Heslop, J., Walter Anthony, K., Winkel, M., Sepulveda-Jauregui, A., Martinez-Cruz, K., Bondurant, A., et al. (2020). A synthesis of methane dynamics in thermokarst lake environments. *Earth-Science Reviews*, *210*, 103365. https://doi.org/10.1016/j.earscirev.2020.103365

Heslop, J. K., Anthony, K. W., Grosse, G., Liebner, S., & Winkel, M. (2019). Century-scale time since permafrost thaw affects temperature sensitivity of net methane production in thermokarst-lake and talik sediments. *Science of the Total Environment*, *691*, 124–134. https://doi.org/10.1016/j.scitotenv.2019.06.402

Hugelius, G., Loisel, J., Chadburn, S., Jackson, R. B., Jones, M., MacDonald, G., et al. (2020). Large stocks of peatland carbon and nitrogen are vulnerable to permafrost thaw. *Proceedings of the National Academy of Sciences*, *117*(34), 20438–20446. https://doi.org/10.1073/pnas.1916387117

In 'T Zandt, M. H., Liebner, S., & Welte, C. U. (2020). Roles of Thermokarst Lakes in a warming world. *Trends in Microbiology*, *28*(9), 769–779. https://doi.org/10.1016/j.tim.2020.04.002

Karlgård, J. (2008). Degrading palsa mires in northern Europe: Changing vegetation in an altering climate and its potential impact on greenhouse gas fluxes. *Lunds universitets Naturgeografiska institution-Seminarieuppsatser*.

Kieser, S., Brown, J., Zdobnov, E. M., Trajkovski, M., & McCue, L. A. (2020). Atlas: A snakemake workflow for assembly, annotation, and genomic binning of metagenome sequence data. *BMC Bioinformatics*, *21*, 1–8. https://doi.org/10.1186/s12859-020-03585-4

Kirkwood, A., Roy-Léveillée, P., Packalen, M. S., McLaughlin, J., & Basiliko, N. (2019). Evolution of palsas and peat plateaus in the hudson bay lowlands: Permafrost degradation and the production of greenhouse gases. *Cold Regions Engineering*, 2019. Retrieved from https://api.semanticscholar.org/CorpusID:214103536

Knoblauch, C., Beer, C., Liebner, S., Grigoriev, M. N., & Pfeiffer, E.-M. (2018). Methane production as key to the greenhouse gas budget of thawing permafrost. *Nature Climate Change*, *8*(4), 309–312. https://doi.org/10.1038/s41558-018-0095-z

Kuhn, M., Lundin, E. J., Giesler, R., Johansson, M., & Karlsson, J. (2018). Emissions from thaw ponds largely offset the carbon sink of northern permafrost wetlands. *Scientific Reports*, *8*(1), 9535. https://doi.org/10.1038/s41598-018-27770-x

Langmead, B., & Salzberg, S. L. (2012). Fast gapped-read alignment with bowtie 2. *Nature Methods*, *9*(4), 357–359. https://doi.org/10.1038/nmeth.1923

Laurent, M., Baysinger, M., Sanders, T., & Treat, C. (2026). Nitrogen species concentrations during a thaw simulation in a permafrost peatland [dataset]. *finland*. https://doi.org/10.5281/zenodo.18594210

Laurent, M., Baysinger, M. R., Schaller, J., Lück, M., Hoffmann, M., Windirsch, T., et al. (2025). Enhanced co2 emissions driven by flooding in a simulation of palsa degradation. *Biogeosciences*, *22*(23), 7881–7899. https://doi.org/10.5194/bg-22-7881-2025

Laurent, M., Lück, M., & Treat, C. C. (2023a). Continuous CO2, CH4 and H2O fluxes measured during a 3-month mesocosm incubation from a palsa [dataset]. *PANGAEA*. https://doi.org/10.1594/PANGAEA.974304

Laurent, M., Lück, M., & Treat, C. C. (2023b). Continuous CO_2, CH_4 and H_2O fluxes measured during a 3-month mesocosm incubation from a palsa [dataset]. *PANGAEA*. https://doi.org/10.1594/PANGAEA.974302

Lee, H., Schuur, E. A. G., Inglett, K. S., Lavoie, M., & Chanton, J. P. (2012). The rate of permafrost carbon release under aerobic and anaerobic conditions and its potential effects on climate. *Global Change Biology*, *18*(2), 515–527. https://doi.org/10.1111/j.1365-2486.2011.02519.x

Leppiniemi, O. (2025). Palsa mires of the northern hemisphere: Environmental characteristics, degradation, and morpho-ecological state. *Nordia Geographical Publications*, *54*(3), 1–63. https://doi.org/10.30671/nordia.161627

Leroy, M., Burnett, M. S., Laurion, I., Douglas, P. M., Kallenbach, C. M., & Comte, J. (2025). Terrestrial-aquatic connectivity structures microbial communities during the formation of thermokarst lakes. *ISME Communications*, *5*(1), ycaf027. https://doi.org/10.1093/ismeco/ycaf027

Li, J., Huang, Y., Wang, J., Zhang, Y., & Chen, Y. (2025). Vermiculite changed greenhouse gases emission and microbial community succession in vermicomposting: Particle size investigation. *Bioresource Technology*, *416*, 131769. https://doi.org/10.1016/j.biortech.2024.131769
Love, M. I., Huber, W., & Anders, S. (2014). Moderated estimation of fold change and dispersion for rna-seq data with deseq2. *Genome Biology*, *15*(12), 1–21. https://doi.org/10.1186/s13059-014-0550-8
Mackelprang, R., Burkert, A., Haw, M., Mahendrarajah, T., Conaway, C. H., Douglas, T. A., & Waldrop, M. P. (2017). Microbial survival strategies in ancient permafrost: Insights from metagenomics. *The ISME journal*, *11*(10), 2305–2318. https://doi.org/10.1038/ismej.2017.93
Mackelprang, R., Saleska, S. R., Jacobsen, C. S., Jansson, J. K., & Taş, N. (2016). Permafrost meta-omics and climate change. *Annual Review of Earth and Planetary Sciences*, *44*(1), 439–462. https://doi.org/10.1146/annurev-earth-060614-105126
Mackelprang, R., Waldrop, M. P., DeAngelis, K. M., David, M. M., Chavarria, K. L., Blazewicz, S. J., et al. (2011). Metagenomic analysis of a permafrost microbial community reveals a rapid response to thaw. *Nature*, *480*(7377), 368–371. https://doi.org/10.1038/nature10576
Malmer, N., Johansson, T., Olsrud, M., & Christensen, T. R. (2005). Vegetation, climatic changes and net carbon sequestration in a North-scandinavian subarctic mire over 30 years. *Global Change Biology*, *11*(11), 1895–1909. https://doi.org/10.1111/j.1365-2486.2005.01042.x
Markkula, I., Turunen, M., & Rasmus, S. (2019). A review of climate change impacts on the ecosystem services in the saami homeland in Finland. *Science of the Total Environment*, *692*, 1070–1085. https://doi.org/10.1016/j.scitotenv.2019.07.272
Maron, P.-A., Sarr, A., Kaisermann, A., Lévêque, J., Mathieu, O., Guigue, J., et al. (2018). High microbial diversity promotes soil ecosystem functioning. *Applied and Environmental Microbiology*, *84*(9). https://doi.org/10.1128/aem.02738-17
Meijboom, F., & van Noordwijk, M. (1991). Rhizon soil solution samplers as artificial roots. In *Root ecology and its practical application* (pp. 793–795). Verein für Wurzelforschung.
Meincke, M., Bock, E., Kastrau, D., & Kroneck, P. M. (1992). Nitrite oxidoreductase from nitrobacter hamburgensis: Redox centers and their catalytic role. *Archives of Microbiology*, *158*(2), 127–131. https://doi.org/10.1007/bf00245215
Melillo, J. M., Butler, S., Johnson, J., Mohan, J., Steudler, P., Lux, H., et al. (2011). Soil warming, carbon–nitrogen interactions, and forest carbon budgets. *Proceedings of the National Academy of Sciences*, *108*(23), 9508–9512. https://doi.org/10.1073/pnas.1018189108
Monteux, S., Keuper, F., Fontaine, S., Gavazov, K., Hallin, S., Juhanson, J., et al. (2020). Carbon and nitrogen cycling in Yedoma permafrost controlled by microbial functional limitations. *Nature Geoscience*, *13*(12), 794–798. https://doi.org/10.1038/s41561-020-00662-4
Nurk, S., Meleshko, D., Korobeynikov, A., & Pevzner, P. A. (2017). Metaspades: A new versatile metagenomic assembler. *Genome Research*, *27*(5), 824–834. https://doi.org/10.1101/gr.213959.116
Obu, J., Westermann, S., Bartsch, A., Berdnikov, N., Christiansen, H. H., Dashtseren, A., et al. (2019). Northern hemisphere permafrost map based on ttop modelling for 2000–2016 at 1 km2 scale. *Earth-Science Reviews*, *193*, 299–316. https://doi.org/10.1016/j.earscirev.2019.04.023
Oksanen, J., Blanchet, F. G., Friendly, M., Kindt, R., Legendre, P., McGlinn, D., et al. (2020). Vegan: Community ecology package [Computer software manual]. Retrieved from https://CRAN.R-project.org/package=vegan(Rpackageversion2.5-7
Oksanen, P. O., Kuhry, P., & Alekseeva, R. N. (2003). Holocene development and permafrost history of the usinsk mire, northeast European Russia. *Géographie Physique et Quaternaire*, *57*(2), 169–187. https://doi.org/10.7202/011312ar
Patzner, M. S., Logan, M., McKenna, A. M., Young, R. B., Zhou, Z., Joss, H., et al. (2022). Microbial iron cycling during Palsa hillslope collapse promotes greenhouse gas emissions before complete permafrost thaw. *Communications Earth and Environment*, *3*(1), 76. https://doi.org/10.1038/s43247-022-00407-8
Patzner, M. S., Mueller, C. W., Malusova, M., Baur, M., Nikeleit, V., Scholten, T., et al. (2020). Iron mineral dissolution releases iron and associated organic carbon during permafrost thaw. *Nature Communications*, *11*(1), 6329. https://doi.org/10.1038/s41467-020-20102-6
Perryman, C. R., McCalley, C. K., Malhotra, A., Fahnestock, M. F., Kashi, N. N., Bryce, J. G., et al. (2020). Thaw transitions and redox conditions drive methane oxidation in a permafrost peatland. *Journal of Geophysical Research: Biogeosciences*, *125*(3), e2019JG005526. https://doi.org/10.1029/2019jg005526
Pester, M. (2012). Sulfate-reducing microorganisms in wetlands – Fameless actors in carbon cycling and climate change. *Frontiers in Microbiology*, *3*. https://doi.org/10.3389/fmicb.2012.00072
Peura, S., Wauthy, M., Simone, D., Eiler, A., Einarsdóttir, K., Rautio, M., & Bertilsson, S. (2020). Ontogenic succession of thermokarst thaw ponds is linked to dissolved organic matter quality and microbial degradation potential. *Limnology & Oceanography*, *65*(S1), S248–S263. https://doi.org/10.1002/lno.11349
Poppeliers, S. W., Hefting, M., Dorrepaal, E., & Weedon, J. T. (2022). Functional microbial ecology in arctic soils: The need for a year-round perspective. *FEMS Microbiology Ecology*, *98*(12), fiac134. https://doi.org/10.1093/femsec/fiac134
Quast, C., Pruesse, E., Yilmaz, P., Gerken, J., Schweer, T., Yarza, P., et al. (2012). The silva ribosomal rna gene database project: Improved data processing and web-based tools. *Nucleic Acids Research*, *41*(D1), D590–D596. https://doi.org/10.1093/nar/gks1219
Rantanen, M., Karpechko, A. Y., Lipponen, A., Nordling, K., Hyvärinen, O., Ruosteenoja, K., et al. (2022). The arctic has warmed nearly four times faster than the globe since 1979. *Communications Earth & Environment*, *3*(1), 168. https://doi.org/10.1038/s43247-022-00498-3
R Core Team. (2021). R: A language and environment for statistical computing [Computer software manual]. Retrieved from https://www.R-project.org/
Reddy, K. R., & DeLaune, R. D. (2008). *Biogeochemistry of wetlands: Science and applications*. CRC Press.
Reddy, K. R., DeLaune, R. D., & Inglett, P. W. (2022). *Biogeochemistry of wetlands: Science and applications*. CRC Press.
Rivkina, E., Shcherbakova, V., Laurinavichius, K., Petrovskaya, L., Krivushin, K., Kraev, G., et al. (2007). Biogeochemistry of methane and methanogenic archaea in permafrost: Methane and methanogenic archaea in permafrost. *FEMS Microbiology Ecology*, *61*(1), 1–15. https://doi.org/10.1111/j.1574-6941.2007.00315.x
Ruppel, M., Väliranta, M., Virtanen, T., & Korhola, A. (2013). Postglacial spatiotemporal peatland initiation and lateral expansion dynamics in North America and northern Europe. *The Holocene*, *23*(11), 1596–1606. https://doi.org/10.1177/0959683613499053
Salmon, V. G., Soucy, P., Mauritz, M., Celis, G., Natali, S. M., Mack, M. C., & Schuur, E. A. (2016). Nitrogen availability increases in a tundra ecosystem during five years of experimental permafrost thaw. *Global Change Biology*, *22*(5), 1927–1941. https://doi.org/10.1111/gcb.13204
Sannel, A. B. K., & Kuhry, P. (2009). Holocene peat growth and decay dynamics in sub-arctic peat plateaus, west-central Canada. *Boreas*, *38*(1), 13–24. https://doi.org/10.1111/j.1502-3885.2008.00048.x
Seppälä, M. (1986). The origin of palsas. *Geografiska Annaler - Series A: Physical Geography*, *68*(3), 141–147.
Serikova, S., Pokrovsky, O., Ala-Aho, P., Kazantsev, V., Kirpotin, S., Kopysov, S., et al. (2018). High riverine co2 emissions at the permafrost boundary of western siberia. *Nature Geoscience*, *11*(11), 825–829. https://doi.org/10.1038/s41561-018-0218-1
Smith, S. L., O'Neill, H. B., Isaksen, K., Noetzli, J., & Romanovsky, V. E. (2022). The changing thermal state of permafrost. *Nature Reviews Earth and Environment*, *3*(1), 10–23. https://doi.org/10.1038/s43017-021-00240-1
Strauss, J., Biasi, C., Sanders, T., Abbott, B. W., von Deimling, T. S., Voigt, C., et al. (2022). A globally relevant stock of soil nitrogen in the yedoma permafrost domain. *Nature Communications*, *13*(1), 6074. https://doi.org/10.1038/s41467-022-33794-9

Strauss, J., Marushchak, M. E., van Delden, L., Sanders, T., Biasi, C., Voigt, C., et al. (2024). Potential nitrogen mobilisation from the yedoma permafrost domain. *Environmental Research Letters*, *19*(4), 043002. https://doi.org/10.1088/1748-9326/ad3167

Strauss, J., Schirrmeister, L., Grosse, G., Fortier, D., Hugelius, G., Knoblauch, C., et al. (2017). Deep yedoma permafrost: A synthesis of depositional characteristics and carbon vulnerability. *Earth-Science Reviews*, *172*, 75–86. https://doi.org/10.1016/j.earscirev.2017.07.007

Su, Y., Zheng, X., Chen, Y., Li, M., & Liu, K. (2015). Alteration of intracellular protein expressions as a key mechanism of the deterioration of bacterial denitrification caused by copper oxide nanoparticles. *Scientific Reports*, *5*(1), 15824. https://doi.org/10.1038/srep15824

Turetsky, M. R., Abbott, B. W., Jones, M. C., Anthony, K. W., Olefeldt, D., Schuur, E. A., et al. (2020). Carbon release through abrupt permafrost thaw. *Nature Geoscience*, *13*(2), 138–143. https://doi.org/10.1038/s41561-019-0526-0

Turetsky, M. R., Wieder, R. K., Williams, C. J., & Vitt, D. H. (2000). Organic matter accumulation, peat chemistry, and permafrost melting in peatlands of boreal Alberta. *Ecoscience*, *7*(3), 115–122. https://doi.org/10.1080/11956860.2000.11682608

Verdonen, M., Störmer, A., Lotsari, E., Korpelainen, P., Burkhard, B., Colpaert, A., & Kumpula, T. (2023). Permafrost degradation at two monitored Palsa mires in north-west Finland. *The Cryosphere*, *17*(5), 1803–1819. https://doi.org/10.5194/tc-17-1803-2023

Voigt, C., Marushchak, M. E., Lamprecht, R. E., Jackowicz-Korczyński, M., Lindgren, A., Mastepanov, M., et al. (2017). Increased nitrous oxide emissions from arctic peatlands after permafrost thaw. *Proceedings of the National Academy of Sciences*, *114*(24), 6238–6243. https://doi.org/10.1073/pnas.1702902114

von Hippel, B., Stoof-Leichsenring, K. R., Çabuk, U., Liu, S., Melles, M., & Herzschuh, U. (2025). Postglacial bioweathering, soil nutrient cycling, and podzolization from palaeometagenomics of plants, fungi, and bacteria. *Science Advances*, *11*(19), eadj5527. https://doi.org/10.1126/sciadv.adj5527

Vonk, J. E., Mann, P. J., Davydov, S., Davydova, A., Spencer, R. G. M., Schade, J., et al. (2013). High biolability of ancient permafrost carbon upon thaw. *Geophysical Research Letters*, *40*(11), 2689–2693. https://doi.org/10.1002/grl.50348

Vonk, J. E., Tank, S. E., Mann, P. J., Spencer, R. G., Treat, C. C., Striegl, R. G., et al. (2015). Biodegradability of dissolved organic carbon in permafrost soils and aquatic systems: A meta-analysis. *Biogeosciences*, *12*(23), 6915–6930. https://doi.org/10.5194/bg-12-6915-2015

Waldrop, M. P., Ernakovich, J. G., Vishnivetskaya, T. A., Schaefer, S. R., Mackelprang, R., Barta, J., et al. (2025). *Microbial ecology of permafrost soils: Populations, processes, and perspectives*. Permafrost and Periglacial Processes.

Waldrop, M. P., Wickland, K. P., White Iii, R., Berhe, A. A., Harden, J. W., & Romanovsky, V. E. (2010). Molecular investigations into a globally important carbon pool: Permafrost-protected carbon in Alaskan soils. *Global Change Biology*, *16*(9), 2543–2554. https://doi.org/10.1111/j.1365-2486.2009.02141.x

Walter Anthony, K., Daanen, R., Anthony, P., Schneider von Deimling, T., Ping, C.-L., Chanton, J. P., & Grosse, G. (2016). Methane emissions proportional to permafrost carbon thawed in Arctic Lakes since the 1950s. *Nature Geoscience*, *9*(9), 679–682. Retrieved 2023-06-12, from https://www.nature.com/articles/ngeo2795doi:10.1038/ngeo2795

Webb, H., Fuchs, M., Abbott, B. W., Douglas, T. A., Elder, C. D., Ernakovich, J. G., et al. (2025). A review of abrupt permafrost thaw: Definitions, usage, and a proposed conceptual framework. *Current Climate Change Reports*, *11*(1), 1–15. https://doi.org/10.1007/s40641-025-00204-3

Wickham, H., Chang, W., Henry, L., Pedersen, T. L., Takahashi, K., Wilke, C., et al. (2024). ggplot2: Elegant graphics for data analysis [Computer software manual]. Retrieved from https://CRAN.R-project.org/package=ggplot2(Rpackageversion3.5.0

Wild, B., Schnecker, J., Knoltsch, A., Takriti, M., Mooshammer, M., Gentsch, N., et al. (2015). Microbial nitrogen dynamics in organic and mineral soil Horizons along a latitudinal transect in Western siberia. *Global Biogeochemical Cycles*, *29*(5), 567–582. https://doi.org/10.1002/2015gb005084

Woodcroft, B. J., Singleton, C. M., Boyd, J. A., Evans, P. N., Emerson, J. B., Zayed, A. A., et al. (2018). Genome-centric view of carbon processing in thawing permafrost. *Nature*, *560*(7716), 49–54. https://doi.org/10.1038/s41586-018-0338-1

Yang, S., Liebner, S., Svenning, M. M., & Tveit, A. T. (2021). Decoupling of microbial community dynamics and functions in arctic peat soil exposed to short term warming. *Molecular Ecology*, *30*(20), 5094–5104. https://doi.org/10.1111/mec.16118